Efficient Hydrodynamic Modulation Voltammetry with a Microcylinder Electrode

Sheila A. Schuette and Richard L. McCreery*

Department of Chemistry, The Ohio State University, Columbus, Ohio 43210

Microcylinder electrodes afford several useful features when combined with hydrodynamic modulation voltammetry (HMV). The small diameter of the vibrating microcylinder electrode results in a low Reynolds number even when the electrode is vibrated at relatively high velocities (13 cm/s). The result is a more laminar flow pattern of the solution around the electrode and an instantaneous current that tracks the electrode velocity. Efficient modulation may be carried out at much higher frequencies than those previously employed in HMV, allowing better discrimination against flicker noise, faster voltammetric scan rates, and easier signal processing. Secondly, the modulation apparatus is simple due to the low mass of the electrode. Finally, the amount of sample consumed is small, permitting the analysis of samples of small volume or low concentration. A detection limit of 3.0×10^{-8} M was obtained for ferrocene in acetonitrile, and excellent rejection of background current for a Pt electrode in aqueous solution was demonstrated.

Hydrodynamic modulation voltammetry (HMV) has shown significant promise for trace analysis, because it significantly reduces interference from background processes normally encountered in electrochemical analysis. These background interferences include capacitive current, surface faradaic reactions, and redox reactions of the electrolyte and are particularly severe on solid electrodes. HMV exploits the fact that the analytical current for a solution species is mass transport controlled, whereas that for most of the background processes is not. The mass transport rate may be modulated by periodic motion of the electrode relative to the solution (or vice versa) to produce an alternating current that depends on freely diffusing analyte concentration, not on surface or electrolyte reactions. By demodulating the ac current at various applied potentials, a voltammogram that is specific to mass transport modulated materials is obtained, with detection limits several orders of magnitude better than conventional voltammetry. Previous reports on HMV have employed electrodes of conventional size (area = ca. 0.1 cm^2) and fairly low (<15 Hz) modulation frequencies. As we report in this paper, there are significant fundamental and practical advantages to using very small (area = ca. 0.001 cm^2) working electrodes, including greater modulation depth, higher useful modulation frequency, and significantly simpler and more compact apparatus.

Hydrodynamic modulation voltammetry and its applications have been reviewed recently by Wang (*1*). The rotating disk electrode (RDE) has been used for HMV, in part because it is one of the few systems for which the hydrodynamic equations and the convective diffusion equation have been solved (*2*). Bruckenstein and Miller and co-workers (*3–7*) have employed the RDE for hydrodynamic modulation voltammetry (HMRDE), whereby the electrode's rotation speed is varied sinusoidally about some center speed at a rate of 3–15 Hz. Although this modulated current is only a fraction of the total current produced, it is free from any contributions from factors that do not depend on the mass transfer rate. Detection limits as low as 5×10^{-9} M have been obtained with this technique (*4*).

In pulsed-rotation voltammetry (PRV) the rotation rate of a RDE is switched between two speeds at a rate <0.1 Hz (*8*). The difference current is then measured at discrete applied potentials, and the voltammogram is plotted pointwise. Blaedel and Engstrom (*8*) reported a detection limit of 1×10^{-8} M for the ferri-/ferrocyanide system.

Blaedel and co-workers have also developed a number of techniques based on flow-through solid electrodes, including stopped- and pulsed-flow and stopped- and pulsed-rotation voltammetry (*9–14*). In the latter technique, the rotation rate of a RDE, immersed in a flowing stream, is switched between two rotation speeds and the difference current is measured. These techniques employ modulation frequencies of 0.1–1 Hz and, except in the case of pulsed-flow voltammetry (*12*), plot the voltammogram in a pointwise fashion after discrete potential changes. Wang and co-workers have developed further variations of stopped-flow and stopped-rotation voltammetry that incorporate potential scanning (*15*, *16*). Detection limits in the nanomolar range have been reported (*11*, *14*).

Vibrating wire electrodes have also been employed for HMV. Pratt and Johnson studied the hydrodynamics of a wire electrode that was vibrated in a reciprocating fashion perpendicular to its axis (*17*, *18*). Both frequency and amplitude modulation were examined and produced equivalent voltammograms, but the instrumental requirements of frequency modulation were more complex. When an amplitude modulation of 10 Hz was used, detection limits of ca. 10^{-8} M were observed. The detection limit was improved (3×10^{-9} M) when the modulation technique was combined with flow injection analysis.

All the techniques described above employ low modulation frequencies. In the case of the HMRDE, it was found that the concentration profile adjusted slowly to a sudden change in the rotation speed compared to the rapid readjustment of the fluid velocity (*5*). Although the theory has been improved to cover a wider range of modulation frequencies (*6*, *19*, *20*), the modulation frequency must be small compared to the center rotation speed to ensure that the modulated component of the current at the fundamental frequency is a significant fraction of the total modulated current. HMV techniques employing stopped or pulsed streams suffer from low modulation frequencies due to the inability to rapidly change the flow rate of the solution through the electrode. Similarly, the modulation frequency of stopped-rotation voltammetry is limited by the inertia and response time of the motor–electrode assembly (*1*). Pratt (*17*) examined the current produced at twice the fundamental vibration frequency of the wire electrode, but its small amplitude precluded its application to analytical determinations, and he modulated the amplitude of the vibration frequency for detection limit studies. Higher modulation frequencies would be desirable for trace voltammetry due to the discrimination against flicker noise at higher frequencies, the easier processing of higher frequency signals, and the ability to employ faster potential scan rates.

0003-2700/86/0358-1778$01.50/0

"Ultramicroelectrodes" having areas less than 0.001 cm^2 have received significant attention in recent years due to their distinct properties compared to conventional electrodes. These include nonplanar diffusion, low time constant, and low ohmic potential error (*21–35*). We report here a new property of ultramicroelectrodes that synergistically improves the performance of HMV. The hydrodynamic properties of small electrodes allow HMV to be carried out at significantly higher modulation frequencies, thus circumventing the common limitation of previous techniques.

EXPERIMENTAL SECTION

The vibration apparatus consisted of a PM mini-shaker type 4810 vibration exciter (Bruel & Kjaer Instruments, Marlborough, MA) driven by a 4-V p–p sine wave produced after amplification from a function generator. The vibrator was subject to a mechanical resonance at about 50 Hz, which disturbed the observed current, and this frequency was avoided. The microcylinder electrode (see below) was held vertically and vibrated perpendicular to its axis. A conventional three-electrode potentiostat based on a summing amplifier was used to control the potential, and the current from the microcylinder electrode was amplified by a Keithley Model 427 current amplifier with a gain of 10^4–10^7 V/A. The current amplifier was operated with a rise time of 0.01 ms. The output from the current amplifier was demodulated by a PARC 186A lock-in amplifier, operated in the 2f mode, at a phase angle of 90° relative to the function generator driving the vibrator. The LIA output (output time constant = 0.1 s) was recorded on an X–Y recorder. Raw current waveforms were recorded with a Textronix 7854 digital scope interfaced to an Apple II^+ microcomputer.

The platinum microcylinder electrodes were constructed by using a flame to collapse glass capillaries onto various diameters (25, 50, and 125 μm) of platinum wire (Goodfellow Metals, Cambridge, England). The glass capillaries were drawn from 2.92-mm-o.d. type 0120 potash soda lead glass (Corning). The electrodes were backfilled with conductive silver epoxy, and a copper wire provided an electrical connection. Larger diameter electrodes were fabricated in a similar fashion from 356- and 810-μm platinum wire. The length of the exposed microcylinder electrodes was approximately 3 mm. The electrodes were cleaned by soaking in concentrated H_2SO_4, followed by rinsing with copious amounts of Nanopure water (Sybron Barnstead, Boston, MA). The reference and auxiliary electrodes were conventional, consisting of an aqueous SCE and a Pt wire.

Ferrocene was obtained from Strem Chemicals (Danvers, MA) and was purified by sublimation according to a published procedure (*36*). Tetrabutylammonium perchlorate (Southwestern Analytical) and high-purity UV grade acetonitrile (Burdick and Jackson) were used as received. 1,1′-Bis(hydroxymethyl)ferrocene (BHMF) was a gift from T. Kuwana.

The amplitude of the vibrating microcylinder electrode was determined with a model FC-14 optical comparator (Jones and Lamson, Springfield, VT). The average velocity was then obtained by multiplying the vibration frequency by twice the peak-to-peak amplitude.

RESULTS AND DISCUSSION

Figure 1 shows the current waveforms obtained when two wire electrodes of different diameter are vibrated sinusoidally. Figure 1A is the raw current waveform obtained from a 25-μm-diameter wire electrode, and Figure 1B is that from a 356-μm-diameter wire electrode, both of which are vibrated at 80 Hz. The peak-to-peak amplitude of the vibration is 0.8 mm, resulting in an average velocity of 13 cm/s. The lower trace in each diagram is the current waveform obtained when the electrode is vibrated at a potential where the redox reaction does not occur. The upper trace is the current waveform that results when the applied potential is held at a value where the oxidation of ferrocene to ferrocinium ion occurs at a diffusion-limited rate.

If one assumes the simplest model of a solution moving past the electrode at some fixed velocity, then the current will be a monotonic function of the fluid velocity. If this model is applied to the present case, the instantaneous current will track the scalar velocity, which is the absolute value of the waveform driving the vibrator, after a 90° phase shift (Figure 2). While this model is oversimplified for the complex case of a cylinder moving at varying velocity, the waveform of Figure 1A does have the approximate shape predicted by the model. As the electrode diameter is increased (Figure 1B), the modulation amplitude decreases significantly relative to the average current, and the waveform resembles a distorted sine wave. In both cases, the observed current is modulated at 160 Hz, which is twice the frequency of the vibrator. The magnitude of the current is smallest at the extremes of the electrode excursion, where the instantaneous velocity is lowest, and greatest near the mean position. It should be noted that the 160-Hz modulation frequency of the current obtained with a microelectrode is much higher than the 1–15-Hz frequencies used in previous approaches and will improve the rejection of flicker noise by the detection electronics.

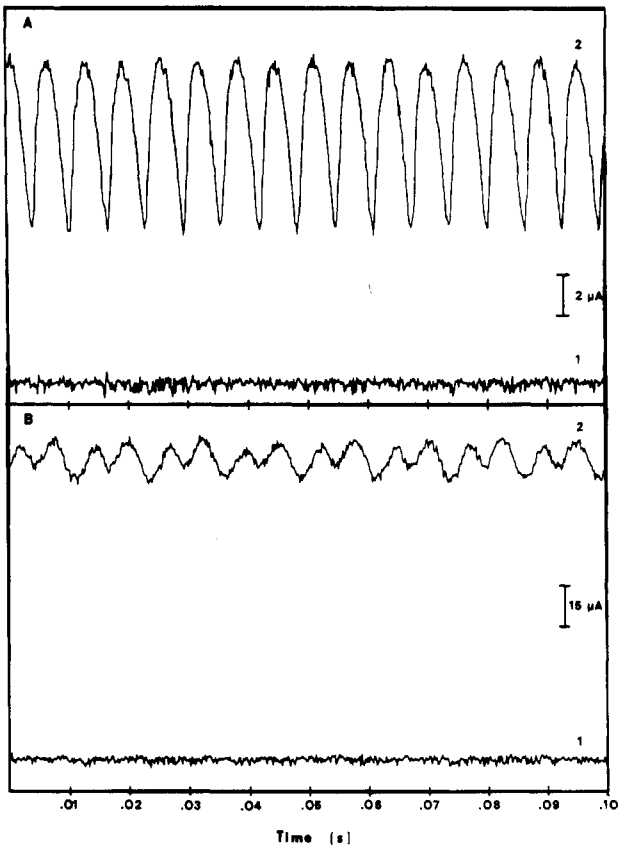

Figure 1. Current waveforms from 0.91 mM ferrocene/0.1 M TBAP in acetonitrile: modulation frequency, 160 Hz; applied potential, 0.0 V vs. SCE (A1, B1) or 0.6 V vs. SCE (A2, B2). (A) 25-μm-Diameter Pt microcylinder electrode: electrode length, 3.0 mm. (B) 356-μm-Diameter Pt wire electrode: electrode length, 3.1 mm.

It is obvious from Figure 1 that the modulated current comprises a much larger fraction of the total current for the smaller diameter electrode. Figure 3 shows the effect of electrode diameter on the modulation efficiency, defined here as the ratio of the p–p amplitude of the ac current to the average current. There is a dramatic increase in the modulation efficiency as the diameter of the wire electrode is decreased below 200 μm. The diameters of the electrodes used by Pratt (*17*) in his vibrating wire experiments were all greater than 300 μm, leading to much smaller modulation efficiencies.

The effect of electrode diameter on modulation efficiency can be understood qualitatively by considering the Reynolds number (Re) (*37*)

$$\mathrm{Re} = Ud_e/\upsilon$$

where U is the velocity of the electrode through the solution,

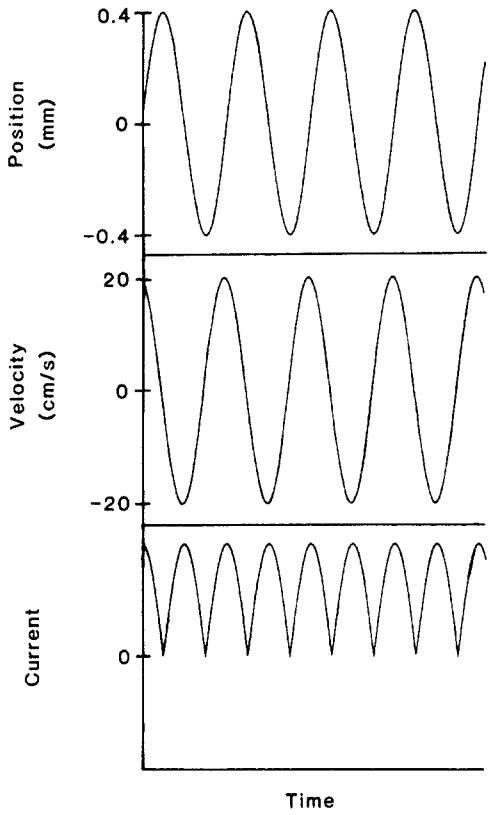

Figure 2. Theoretical position, velocity, and current vs. time for a microcylinder electrode vibrating at 80 Hz. The absolute magnitude of the current depends upon the size and diameter of the microcylinder electrode used.

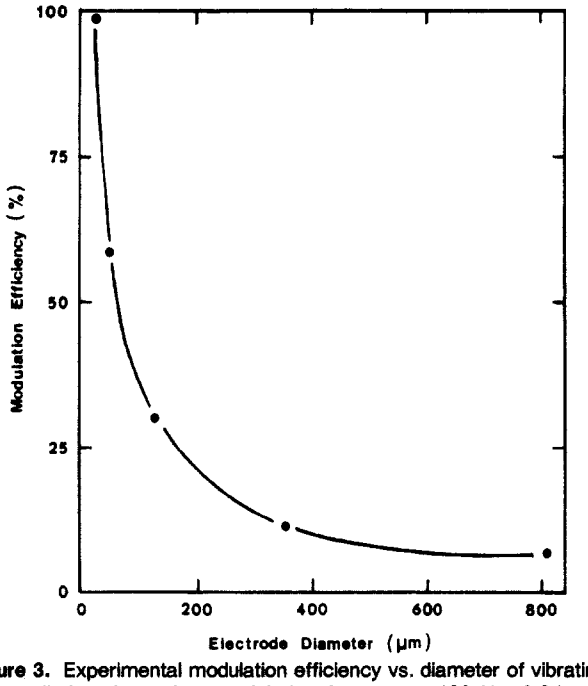

Figure 3. Experimental modulation efficiency vs. diameter of vibrating microcylinder electrode: modulation frequency, 160 Hz; 0.91 mM ferrocene/0.1 M TBAP in acetonitrile.

d_e is the diameter of the electrode, and υ is the kinematic viscosity. The use of a Reynolds number assumes that the vibrating electrode can be considered a cylinder moving through a fluid rather than reciprocating, a reasonable assumption if the vibration amplitude is large relative to the wire diameter. At low values of Re (<1), the flow of solution around the electrode is laminar and symmetric, and the convective mass transport rate is directly related to the velocity of the electrode through the solution. In this case, the

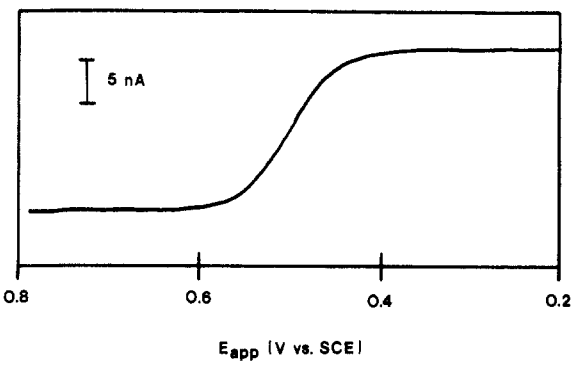

Figure 4. Experimental voltammogram obtained from 5×10^{-6} M ferrocene/0.1 M TBAP in acetonitrile: scan rate, 10 mV/s; electrode diameter, 25 μm; modulation frequency, 160 Hz.

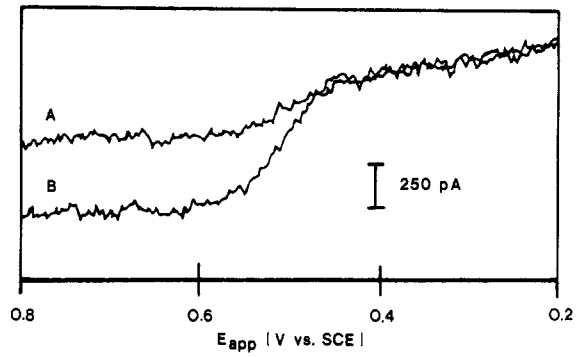

Figure 5. Voltammograms obtained at low concentrations. Conditions are as in Figure 4: (A) 1.1×10^{-7} M ferrocene and (B) 2.1×10^{-7} M ferrocene.

observed instantaneous current is directly dependent on the electrode velocity, and the current will be modulated by a modulation of the electrode velocity. At Re > ~5, separation of the boundary layer occurs behind the electrode, and recirculating eddies are formed. These elongate with increasing Re and eventually break into very irregular flow patterns when Re exceeds about 40 (*38*). For these higher Reynolds numbers, there will not be a direct relationship between current and electrode velocity, and it will be difficult to modulate the current. At a given Re, a smaller electrode will have a higher velocity, and therefore higher vibration frequency. For example, at 80 Hz, a 25-μm-diameter electrode has an average Re of 7.4. For the same Re, a 2-mm-diameter electrode could only be modulated at 1 Hz. The conclusions of this discussion should be considered qualitative, but it is clear that a smaller electrode can be modulated at a higher frequency for a given Re.

The ac current waveforms of Figure 1 may be demodulated by a lock-in amplifier (LIA) to generate a dc output proportional to the ac current. A plot of the LIA output is shown in Figure 4, where the potential was scanned at 10 mV/s. The voltammogram has the sigmoidal shape expected for hydrodynamic voltammetry, with an excellent signal-to-noise ratio for micromolar concentrations. While the magnitude of the current is in the nanoampere to picoampere range for the small (<100 μm) electrodes, such low values are easily measured due to the excellent noise characteristics of synchronous detection. Voltammograms at concentrations near the detection limit are shown in Figure 5. The reference signal for the LIA was provided by the function generator that drives the mini-shaker and was doubled internally by the LIA. The potential was scanned at a rate that was slow relative to both the vibration frequency and the LIA time constant.

Calibration curves of ac signal vs. ferrocene concentration for a 25-μm-diameter microcylinder electrode vibrated at 80 Hz were linear from 3.0×10^{-8} to 1.2×10^{-3} M (slope of log–log

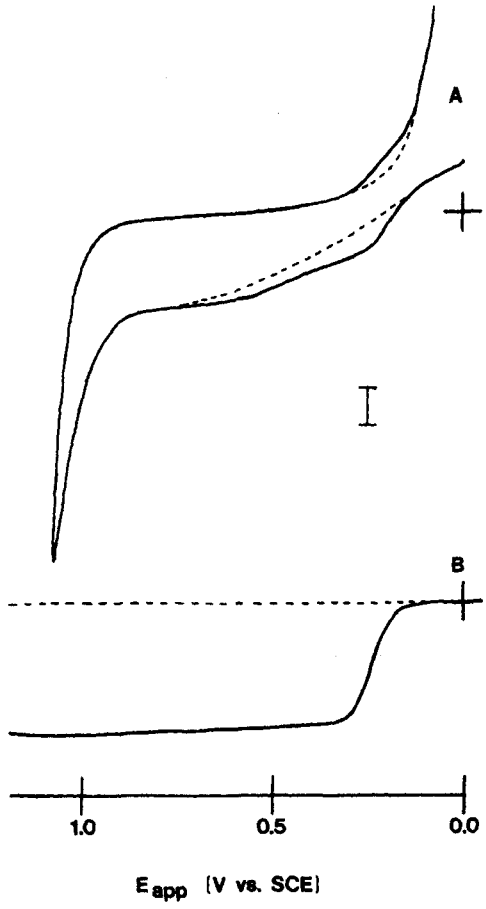

Figure 6. Comparison of a cyclic voltammogram using a conventionally sized Pt disk electrode with a hydrodynamic modulation voltammogram using a microcylinder Pt electrode. Solid lines were obtained from 0.17 mM BHMF in pH 7 citric acid/phosphate buffer, while the dashed lines are of the blank buffer solution: scan rate, 50 mV/s; (A) conventional voltammogram from a 1.5-mm-diameter Pt disk electrode, scale = 1 μA; (B) HMV from a 25-μm-diameter electrode vibrating at 80 Hz, scale = 50 nA.

plot = 0.969, correlation coefficient = 0.995). At 3.0×10^{-8} M, the ratio of signal to the root mean square signal from a blank was 2.0. This detection limit is comparable to those obtained with the HMV techniques cited earlier (*4*, *15–17*).

Figure 6 demonstrates the extent of background rejection with HMV at a microcylinder electrode. All voltammograms were obtained with platinum electrodes in aqueous buffer in the presence and absence of 0.17 mM bis(hydroxymethyl)-ferrocence (BHMF). For a conventional voltammogram (A) from a 1.5-mm-diameter Pt disk, the BHMF signal is barely discernible above the blank. For a microcylinder electrode with hydrodynamic modulation (B), the background is minimal and the BHMF signal is dominant. The background voltammogram remained flat for potentials up to 1.3 V vs. SCE, at which point the increase in dc current caused the current amplifier to overload. The ratio of BHMF signal to background current increases from 2.7 for the Pt disk (measured for the oxidation peak at 0.25 V vs. SCE) to 210 for the microcylinder operated in the HMV mode (measured for the oxidation peak at 0.35 V vs. SCE). This increase in signal-to-background current may be due in part to the enhanced diffusion at the microelectrode, although this effect would not be large for a 25-μm-diameter electrode. A conventional voltammogram using the same electrode in the same solution but without vibration yielded large background currents and a low signal-to-background ratio, indicating that the major enhancement in the signal-to-background ratio resulted from hydrodynamic modulation rather than enhanced diffusion.

Little was gained by using electrodes with diameters smaller than 25 μm. While the modulation efficiency increases with smaller diameter, the area decreases, and the absolute current becomes small enough to introduce noise during amplification. A diameter of 25 μm is a good compromise between hydrodynamic characteristics and absolute signal size. In addition, smaller electrodes are insufficiently stiff to tolerate vibration at the frequencies employed. It should also be noted that microdisk electrodes were unsuitable for these experiments due to very small modulation efficiencies.

The combination of HMV and ultramicroelectrodes results in four analytically useful features. First, the small electrode size yields a low Reynolds number at relatively high electrode velocities. The result is good modulation efficiency at relatively high frequencies, and the reduction of flicker noise in the detection process. In addition, the higher modulation frequency should permit higher voltammetric scan rates. Second, the modulation apparatus is simple due to the low mass of the electrode. High frequencies and electrode velocities may be achieved with low vibration amplitude, light-duty drivers, and small solution volume. Third, the small absolute currents minimize absolute sample consumption, so very low concentrations or small sample volumes are permissible. Fourth, the background signal at a Pt electrode in water is greatly reduced.

ACKNOWLEDGMENT

We thank C. D. Andereck, Department of Physics, The Ohio State University, for helpful discussions and T. Kuwana, Center for Bioanalytical Research, University of Kansas, for the gift of BHMF.

Registry No. BHMF, 1291-48-1; ferrocene, 102-54-5.

LITERATURE CITED

(1) Wang, J. *Talanta* **1981**, *28*, 369–376.
(2) Bard, A. J.; Faulkner, L. R. *Electrochemical Methods*; Wiley: New York, 1980.
(3) Miller, B.; Bruckenstein, S. *J. Electrochem. Soc.* **1974**, *121*, 1558–1562.
(4) Miller, B.; Bruckenstein, S. *Anal. Chem.* **1974**, *46*, 2026–2033.
(5) Tokuda, K.; Bruckenstein, S.; Miller, B. *J. Electrochem. Soc.* **1975**, *122*, 1316–1322.
(6) Tokuda, K.; Bruckenstein, S.; Miller, B. *J. Electrochem. Soc.* **1979**, *126*, 431–436.
(7) Kanzaki, Y.; Bruckenstein, S. *J. Electrcohem. Soc.* **1979**, *126*, 437–441.
(8) Blaedel, W. J.; Engstrom, R. C. *Anal. Chem.* **1978**, *50*, 476–479.
(9) Blaedel, W. J.; Boyer, S. L. *Anal. Chem.* **1971**, *43*, 1538–1540.
(10) Blaedel, W. J.; Iverson, D. G. *Anal. Chem.* **1977**, *49*, 1563–1566.
(11) Blaedel, W. J.; Wang, J. *Anal. Chem.* **1979**, *51*, 799–802.
(12) Blaedel, W. J.; Yim, Z. *Anal. Chem.* **1980**, *52*, 564–566.
(13) Blaedel, W. J.; Wang, J. *Anal. Chim. Acta* **1980**, *116*, 315–322.
(14) Blaedel, W. J.; Wang, J. *Anal. Chem.* **1980**, *52*, 1697–1700.
(15) Wang, J.; Dewald, H. D. *Anal. Chim. Acta* **1982**, *136*, 77–84.
(16) Wang, J.; Freiha, B. A. *Analyst (London)* **1983**, *108*, 685–690.
(17) Pratt, K. W., Jr. Ph.D. Thesis, Iowa State University, 1981.
(18) Pratt, K. W., Jr.; Johnson, D. C. *Electrochim. Acta* **1982**, *27*, 1013–1021.
(19) Deslouis, C.; Gabrielli, C.; Sainte-Rose Fanchine, Ph.; Tribollet, B. *J. Electrochem. Soc.* **1982**, *129*, 107–118.
(20) Tribollet, B.; Newman, J. *J. Electrochem.* Soc. **1983**, *130*, 2016–2026.
(21) Bindra, P.; Brown, A. P.; Fleischmann, M.; Pletcher, D. *J. Electroanal. Chem.* **1975**, *58*, 31–37, 39–50.
(22) Dayton, M. A.; Brown, J. C.; Stutts, K. J.; Wightman, R. M. *Anal. Chem.* **1980**, *52*, 946–950.
(23) Dayton, M. A.; Ewing, A. G.; Wightman, R. M. *Anal. Chem.* **1980**, *52*, 2392–2396.
(24) Scharifker, B.; Hills, G. J. *J. Electroanal. Chem.* **1981**, *130*, 81–97.
(25) Wightman, R. M. *Anal. Chem.* **1981**, *53*, 1125A–1134A.
(26) Ewing, A. G.; Dayton, M. A.; Wightman, R. M. *Anal. Chem.* **1981**, *53*, 1842–1847.
(27) Robinson, R. S.; McCurdy, C. W.; McCreery, R. L. *Anal. Chem.* **1982**, *54*, 2356–2361.
(28) Hepel, T.; Osteryoung, J. *J. Phys. Chem.* **1982**, *86*, 1406–1411.
(29) Howell, J. O.; Wightman, R. M. *Anal. Chem.* **1984**, *56*, 524–529.
(30) Bond, A. M.; Fleischmann, M.; Robinson, J. *J. Electroanal. Chem.* **1984**, *168*, 299–312.
(31) Aoki, K.; Akimoto, K.; Tokuda, K.; Matsuda, H.; Osteryoung, J. *J. Electroanal. Chem.* **1984**, *171*, 219–230.
(32) Bond, A. M.; Fleischmann, M.; Robinson, J. *J. Electroanal. Chem.* **1984**, *180*, 257–263.
(33) Robinson, R. S.; McCreery, R. L. *J. Electroanal. Chem.* **1985**, *182*, 61–72.

(34) Howell, J. O.; Wightman, R. M. J. Phys. Chem. 1984, 88, 3915-3918.
(35) Schuette, S. A.; McCreery, R. L. J. Electroanal. Chem. 1985, 191, 329-342.
(36) Jolly, W. J. The Synthesis and Characterization of Inorganic Compounds; Prentice Hall: Englewood Cliffs, NJ, 1970; p 486.
(37) Adams, R. N. Electrochemistry at Solid Electrodes; Marcel Dekker: New York, 1969.
(38) Van Dyke, M. An Album of Fluid Motion; Parabolic: Stanford, 1982; pp 20, 28-31.

RECEIVED for review January 21, 1986. Accepted March 25, 1986. This work was supported by the Chemical Analysis division of the National Science Foundation.

Carbon-Ring Electrodes with 1-μm Tip Diameter

Yeon-Taik Kim, Donald M. Scarnulis, and Andrew G. Ewing*

Department of Chemistry, The Pennsylvania State University, University Park, Pennsylvania 16802

The successful fabrication of ultrasmall ring-shaped electrodes with tip diameters as small as 1 μm is reported. These electrodes are formed by pyrolysis of methane inside of hot quartz micropipettes. The tip is filled with epoxy and cleaved to expose a ring-shaped carbon electrode. The small total dimension of these electrodes should make them unique for voltammetric measurements in ultrasmall environments. Voltammograms obtained at these electrodes are sigmoidal at low scan rates (<1 V/s), and the limiting current can be approximated by the equation derived for a spherical correction to a hemispherical electrode ($i_l = 2\pi rnFDC$). Apparent charge transfer kinetics for ferricyanide reduction are slowed at these electrodes, and these phenomena are discussed in relation to the carbon film and the effect of electrode dimension. Finally, these electrodes demonstrate a large degree of selectivity for the oxidation of dopamine in the presence of ascorbic acid and are useful for trace determination of dopamine to the micromolar level.

There has been a large amount of interest recently in the development of ultrasmall electrodes for voltammetry (*1-7*). Ultrasmall voltammetric electrodes have several unique properties. At low scan rates (<1 V/s) linear scan voltammograms at these electrodes are sigmoidal in shape (*1, 2, 4*). This behavior is the result of "edge" diffusion and also causes ultrasmall electrodes to be "blind" to all but very fast chemical reactions following charge transfer (*8, 9*). In addition, "edge" diffusion results in a diffusion-limited current at a disk electrode that is proportional to the electrode radius rather than the area. This in turn provides an electrochemical response with small electrodes that has a relatively small component from capacitive charging currents (*10, 11*). Finally, the small currents passed when ultrasmall electrodes are used permit electroanalysis in highly resistive solutions with a minimal effect from potential drop across the electrochemical cell (*2, 4, 11-13*). The combination of small capacitive charging current and small potential drop across uncompensated cell resistance provides a system where high-scan-rate cyclic voltammetry is possible (*11, 14*). Scan rates as high as 100 000 V/s have been achieved (*11*).

Several investigators have predicted theoretically that the apparent rate of charge transfer between analyte and electrode should decrease at ultrasmall electrodes (*8, 15*). Dayton et al. predicted this effect at disk-shaped electrodes for diameters in the 0.1-1-μm range (*8*). Fleischmann et al. have provided a theoretical description of charge transfer at thin-ring electrodes (*15*). Early experimental results have provided evidence for this effect. Wightman and co-workers have demonstrated a reduced apparent charge transfer rate constant for ferricyanide reduction at ultrathin band-shaped electrodes (*16*). Another ultrathin electrode is the thin-ring electrode developed by McFarlane and Wong (*17*) using vapor deposition and sputtering of gold and platinum, respectively.

One interesting aspect to ultrasmall electrodes is that a few of these electrodes have small structural supports as well as small electroactive areas. Electrodes with tip diameters as small as 20 μm have been fabricated from carbon fibers sealed with epoxy in glass micropipettes (*18*). In addition to the disk-shaped carbon fiber electrodes, cylindrical-shaped electrodes with diameters as small as that of a carbon fiber (down to ~6 μm) have been characterized (*6*). Although cylindrical electrodes have a small diameter, problems associated with cutting the fibers necessitate the carbon fiber being tens to hundreds of micrometers long.

Structurally small electrodes can be useful for electroanalysis in extremely small enviroments. These enviroments might include samples of extremely exotic solvents, corrosion pits on metals, pores within heterogeneous polymer membranes, the ends of capillary liquid chromatography columns, and the cytoplasm of living cells. Most of these applications require electrodes with tip dimension on the order of a few micrometers or less. This is especially true for puncturing living cells where the cell membrane must seal around the electrode following implantation.

Carbon deposition by hydrocarbon pyrolysis has been used to fabricate electrode surfaces. In 1964, Beilby et al. pyrolyzed methane over a heated ceramic rod to produce a carbon electrochemical substrate (*19*). The charge transfer properties of these carbon-film electrodes were judged better than wax-impregnated graphite electrodes, but inferior to the platinum electrode. More recently, Blaedel and Mabbott pyrolyzed methane over hot quartz rods to form disk-shaped carbon-film electrodes (*20*). Ferricyanide reduction at these carbon-film electrodes was electrochemically irreversible but improved dramatically following an electrochemical treatment involving cycling between high potentials.

We describe here the successful fabrication of carbon electrodes with total structural tip diameters as small as 1 μm. These experiments were carried out by pyrolysis of methane inside of pulled quartz capillaries. The resultant pyrolytic carbon forms a film on the inside of the capillary and, after filling with epoxy, the electrode geometry is that of a microring. Although the method of carbon deposition is similar

0003-2700/86/0358-1782$01.50/0